

Supplementary Information

Interfacial stabilization of quantum dot/liquid crystal co-assemblies for efficient circularly polarized luminescence

Junlong Xiao, Qiulian Liu, Qinglong Tu, Muhammad Umer, Nan Ren, Qiang Jing*, Haiguang Zhao*, Yang Song*

College of Physics, State Key Laboratory of Bio-Fibers and Eco-Textiles, College of Textiles & Clothing, Qingdao University, No. 308 Ningxia Road, Qingdao 266071, P.R. China.

*Corresponding authors. E-mail: jingq@qdu.edu.cn (Q.J.); hgzhao@qdu.edu.cn (H.Z.); yangsong@qdu.edu.cn (Y.S.)

Experimental Methods

Materials

Cadmium oxide, Zinc acetate, Selenium, Sulfur, 1-Octadecene, Oleic acid (OA), Trioctylphosphine (TOP), Phenyl Stearate, Toluene, reactive mesogen 2-Methyl-1,4-phenylene bis(4-(3-(acryloyloxy)propoxy)benzoate) (RM257), chiral dopant LC756 were all purchased from Aladdin Chemical Co., Ltd., Shanghai, China. All chemicals were used as received.

Synthesis and ligands exchange of quantum dots

0.4 mmol CdO, 4 mmol Zn(AC)₂, 17.6 mmol oleic acid (OA), and 20 mL 1-octadecene (ODE) were placed in a 100 mL round-bottom flask. The mixture was heated to 150 °C and degassed for 20 minutes, followed by purging with N₂ gas. The temperature was then raised to 310 °C to form a clear solution of Cd(OA)₂ and Zn(OA)₂. At this temperature, a solution of 0.4 mmol Se and 4 mmol S in 3 mL tri-n-octylphosphine (TOP) was swiftly injected into the reaction flask. After 1 minute of reaction, the system was cooled to room temperature. Two 5 mL portions of the quantum dot solution with a concentration of 20 mg/mL were transferred to glass vials, to which 10 mmol OA and 10 mmol TOP were added separately. The mixtures were heated to 120 °C and stirred for 36 h. The quantum dots were washed three cycles with toluene and methanol, and finally redispersed in toluene for storage.

Preparation of co-assembly film

500 mg of RM257, 25 mg of LC756, and 15 mg of phenyl stearate were placed in a glass vial. Then add 1 mL of toluene and heat it to 60 °C until the solution becomes transparent. Subsequently, 1 mL of 20 mg/mL quantum dots toluene solution was added. The mixture was heated to 120 °C until the toluene completely evaporated. The precursor was then poured into a liquid crystal cell (composed of two identical glass slides and a 25 μm thick spacer). UV photopolymerization was carried out at 90 °C for 5 minutes, after which the liquid crystal cell was removed to obtain the CLC film. For the preparation of CLC film with dolphin pattern, UV photopolymerization was first performed at 90 °C through a photomask after pouring the precursor into the liquid crystal cell. The mask was then removed, followed by a second round of UV photopolymerization at 25 °C.

Characterization

The lattice structure of the synthesized CdSe/ZnS quantum dots was characterized by transmission electron microscopy (TEM, JEOL, JEM-2100 F) at an accelerating voltage of 200 kV. The elemental composition and functional groups of the ligand-exchanged quantum dots were analyzed using X-ray photoelectron spectroscopy (XPS, Axis Supra+) and Fourier-transform infrared spectroscopy (FTIR, ESCALAB Xi+, Thermo Fisher Scientific). Fluorescence microscopy images of the quantum dot/liquid crystal co-assemblies were obtained with a fluorescence microscope (BX53, Olympus Corporation). The circularly polarized luminescence (CPL) and circular dichroism (CD) of the cholesteric liquid crystal films were characterized using a CPL measurement system (CPL-300, JASCO Corporation) and a CD spectrometer (J-1500, JASCO Corporation), respectively. The reflection artifacts are avoided by removing the substrate and detecting the pure co-assembly films. The fluorescence and reflection spectra were measured with a micro-fiber optic spectrometer (USB200+, Ocean Optics).

Calculation

The circular dichroism (CD) is calculated by $CD = 32980 \times (AL - AR)$, where AL and AR represent the absorbance of left-handed and right-handed circularly polarized light for the sample, respectively. The CPL is calculated by $CPL = 32980 \times ((I_L - I_R) / 2I_A)$, where I_A denotes the average light intensity (I_A)

corresponding to the direct current (DC) component collected by the JASCO CPL-300 circularly polarized fluorescence spectrometer during the measurement process. The g_{lum} is calculated by $g_{lum} = 2 \times (I_L - I_R) / (I_L + I_R)$, where I_L and I_R represent the intensities of the left and right circularly polarized emissions, respectively. The coefficient $32980 \approx 1000 \times (180 \times \ln 10) / 4\pi$, converting the detected absorbance of instruments to ellipticity.

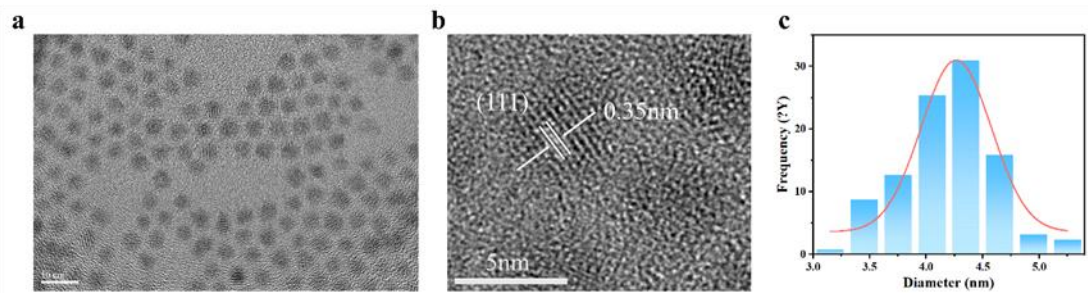


Figure S1. TEM micrographs (a, b) and size distribution histogram (c) of the CdSe/ZnS quantum dots.

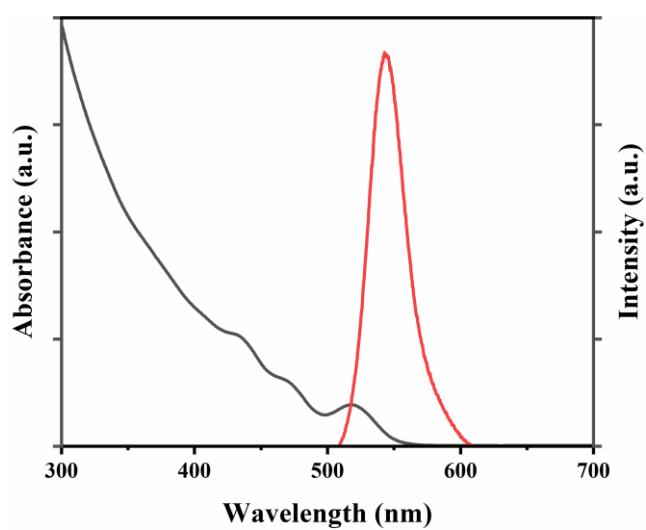


Figure S2. The absorption and emission spectra of quantum dots.

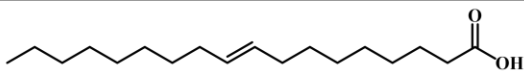
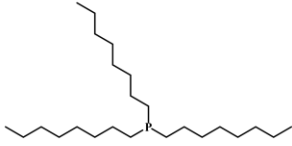
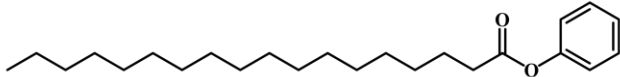
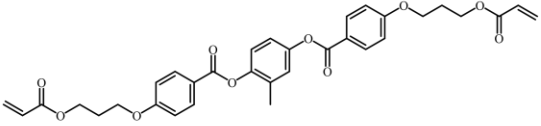
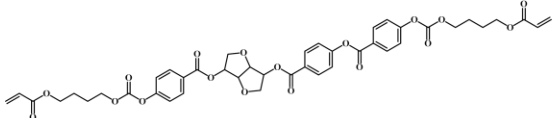
OA	
TOP	
PS	
RM257	
LC756	

Figure S3. Chemical structural formulas of the key compounds used in this study.

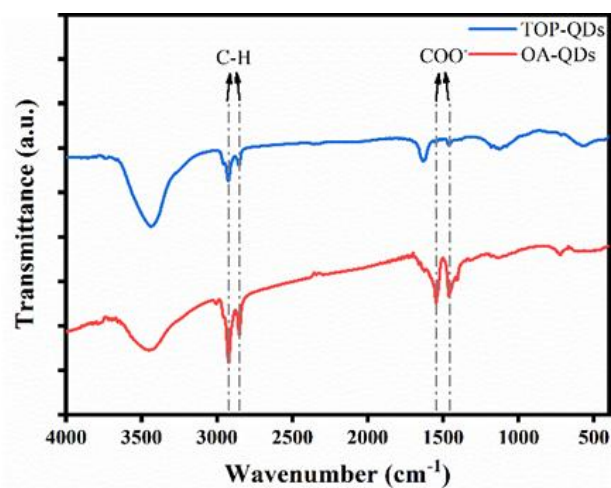


Figure S4. Fourier-transform infrared (FTIR) spectra of the quantum dots after ligand exchange.

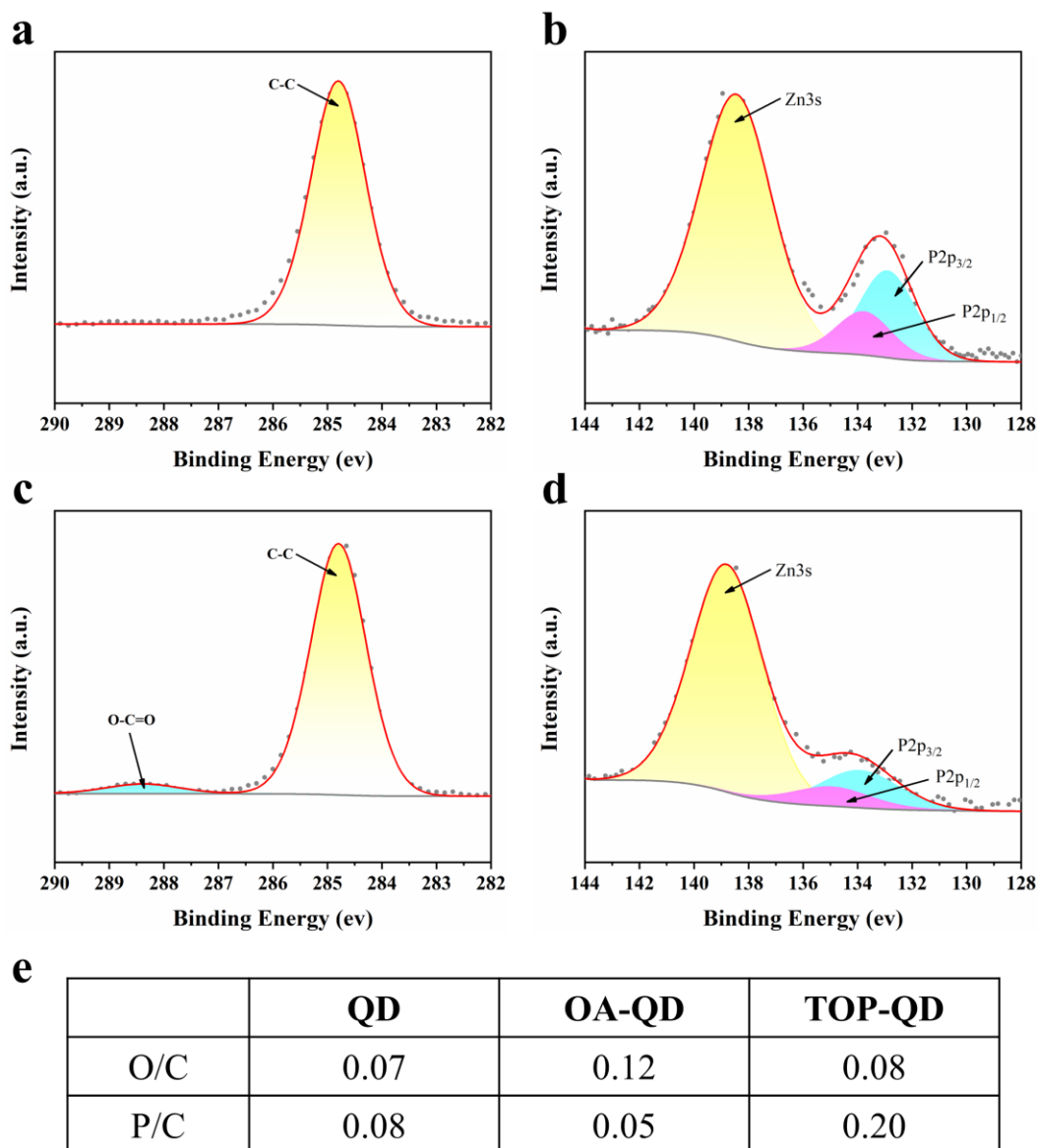


Figure S5. X-ray photoelectron spectroscopy (XPS) analysis of the quantum dots after ligand exchange. (a, b) High-resolution C 1s and P 2p spectra of TOP-QDs; (c, d) High-resolution C 1s and P 2p spectra of OA-QDs; (e) Quantitative XPS element ratios (P/C, O/C) before and after ligand exchange.

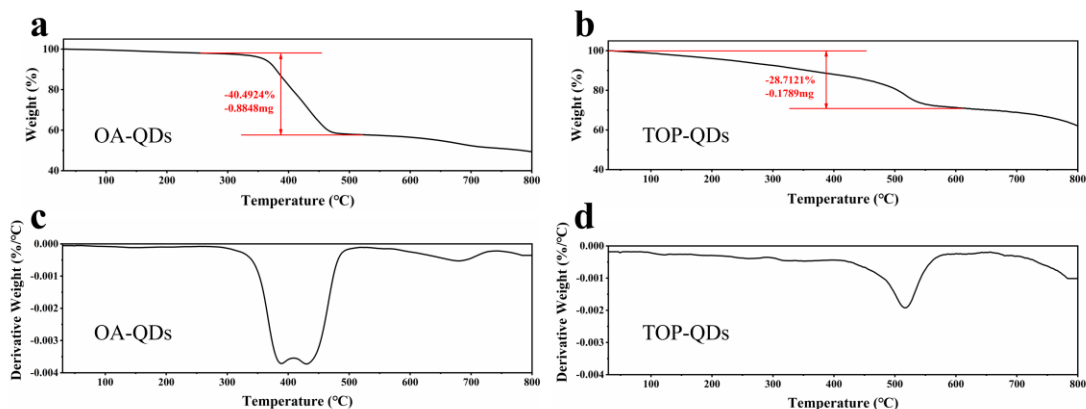


Figure S6. Thermogravimetry (TG) analysis of the quantum dots after ligand exchange. (a, c) TG and DTG spectra of OA-QDs; (b, d) TG and DTG spectra of TOP-QDs. The TG curve shows the ligand contents of OA-QDs and TOP-QDs are 40.5% and 28.7%, respectively.

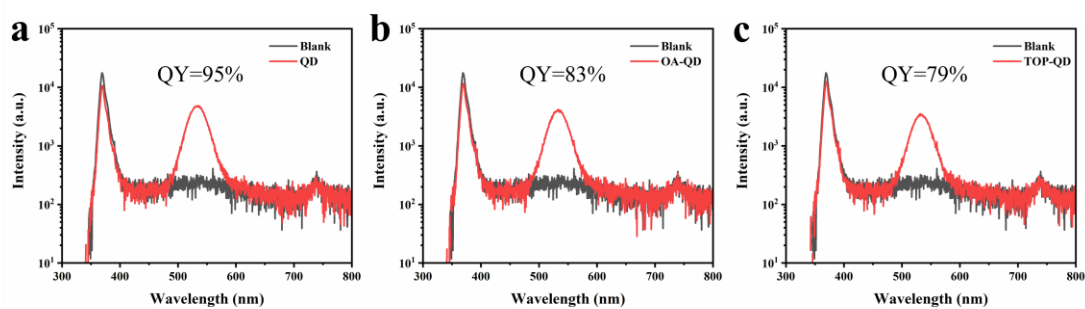


Figure S7. The PLQY of QDs before and after ligand exchange. (a) The PLQY of QDs before ligand exchange; (b, c) The PLQY of OA-QDs and TOP-QDs. All the PLQYs were measured by the Ocean Optics integrating sphere system.

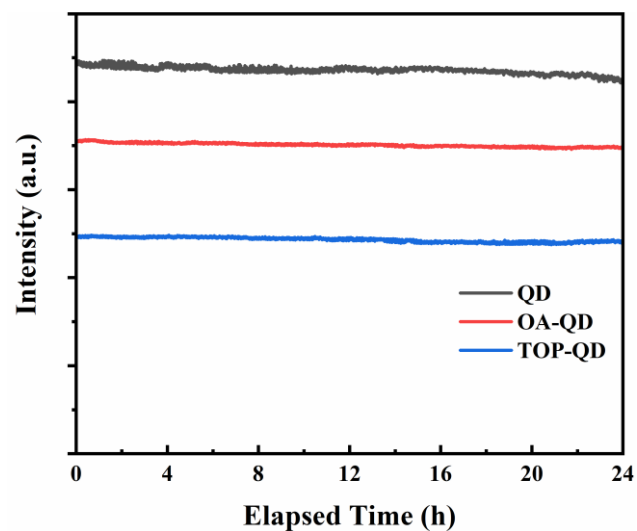


Figure S8. The photoluminescence stability of QDs before and after ligand exchange.

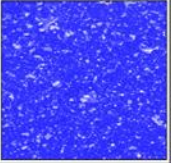
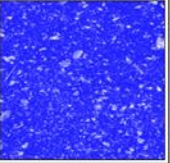
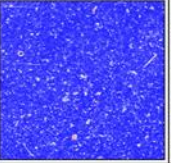
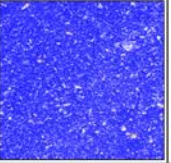
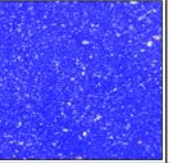
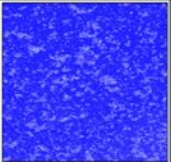
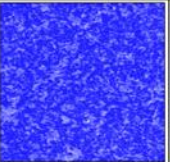
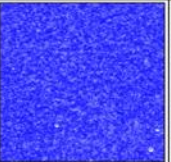
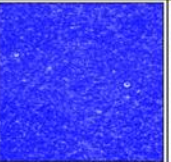
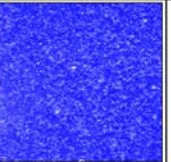
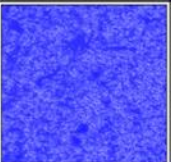
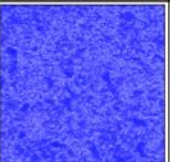
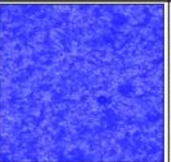
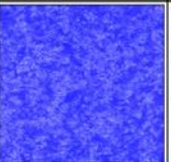
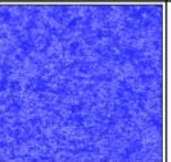
		1	2	3	4	5	Mean
OA-QDs	Heat Map						
	CV	0.47	0.49	0.52	0.51	0.43	0.48
TOP-QDs	Heat Map						
	CV	0.37	0.39	0.34	0.35	0.40	0.37
PS-QDs	Heat Map						
	CV	0.25	0.26	0.26	0.26	0.27	0.26

Figure S9. Statistics of multiple areas of OA-QD, TOP-QD and PS-QD.

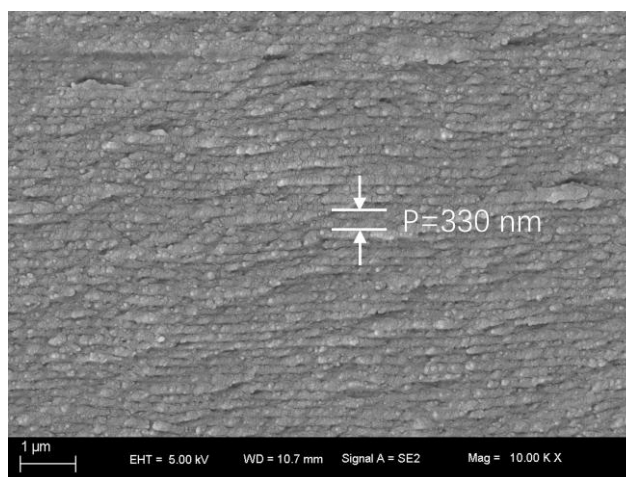


Figure S10. The cross-section SEM image of co-assembly film.

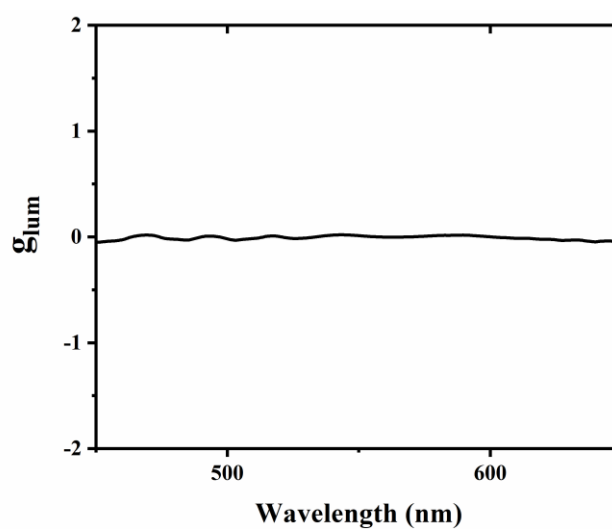


Figure S11. The g_{lum} spectrum of non-assembled sample, which is photopolymerized at temperatures above the liquid crystal critical temperature.

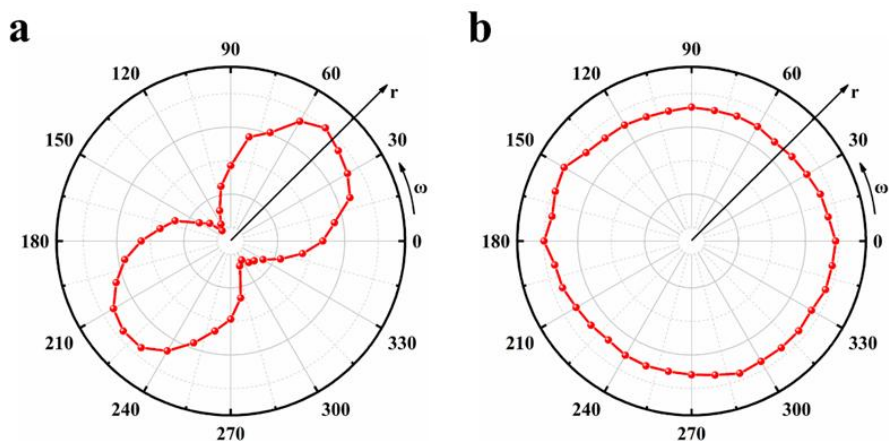


Figure S12. Emission intensity of the co-assembly film as a function of polarizer angle, with the quarter-wave plate installed and removed, where ω represents the transmission angle of the polarizer and r represents the transmittance.

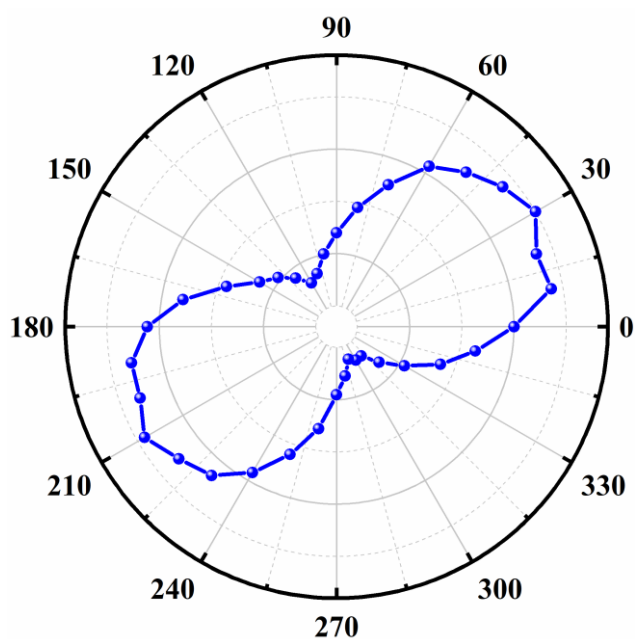


Figure S13. The performance of linearly polarized luminescent film made by co-assembly. Apart from the absence of chiral dopants, this film shares the same composition as CPL film and is directionally assembled via friction alignment method.

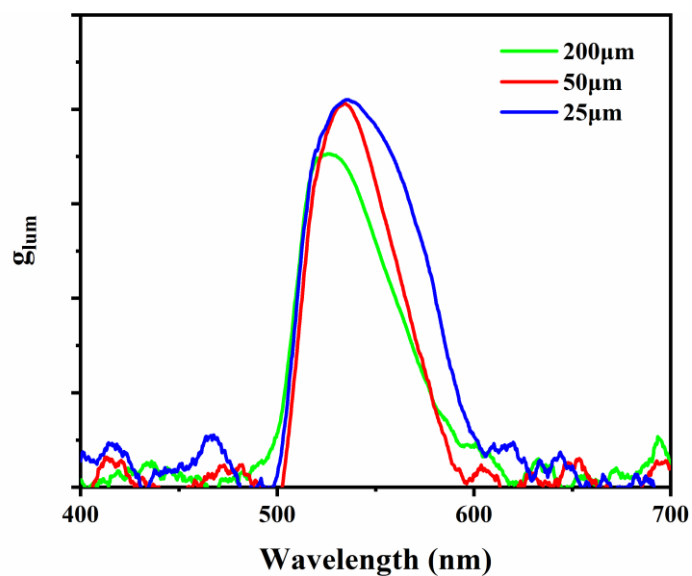


Figure S14. The g_{lum} of co-assembly films with different thickness. The smaller g_{lum} value of 200 μm thick film indicates more structural defects in it.

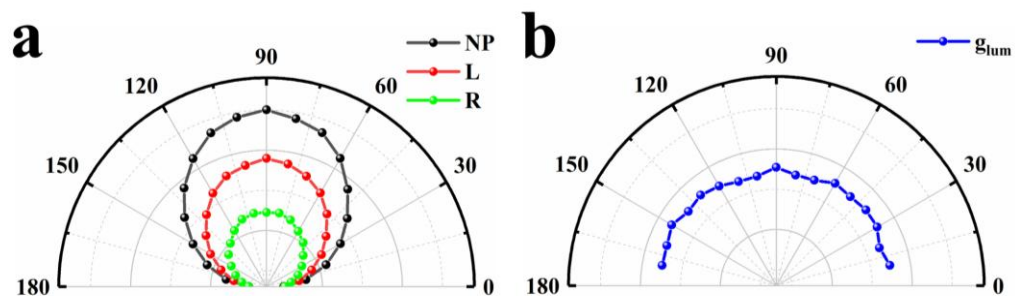


Figure S15. (a) The angle-dependent emission intensity and (b) the angle-dependent g_{lum} of co-assembly film. NP, L and R represent the non-polarization, left-hand polarization and right-hand polarization, respectively.

Table S1. Performance statistics for solid-state QDs-CLC co-assembly materials.

Emitter	CPL (mdeg)	CD (mdeg)	g_{lum}	References
CdSe/ZnS	6000	-28000	1.1	This work
CdSe/ZnS	± 150000		-0.484 and 0.350	Guo Y, Ye Z, Cui Y, et al. Dual Mode Circularly Polarized Luminescence Enabled by Spray Deposition Quantum Dots on a Porous Cholesteric Liquid Crystal Template[J]. <i>Small</i> , 2026: e14016.
CdSe/ZnS			-0.2318	Liu X, Zola R S, Chen Y, et al. Strain-Responsive Circularly Polarized Luminescence in Cholesteric Liquid Crystal Elastomers through Laser-Engineered Microstructures[J]. <i>Advanced Functional Materials</i> , 2025: e28997.
CdSe/ZnS	-1200		-0.74	Li S, Tang Y, Fan Q, et al. When quantum dots meet blue phase liquid crystal elastomers: visualized full-color and mechanically-switchable circularly polarized luminescence[J]. <i>Light: Science & Applications</i> , 2024, 13(1): 140.
CdSe/ZnS	1200		1.0	Han D, Peng L, Chen G, et al. Light-driven energy transfer in luminescent helical superstructures coassembled by inorganic and organic molecules[J]. <i>Chemistry of Materials</i> , 2024, 36(8): 3786-3793.
CdSe/ZnS	± 1800	16000	0.35	Yu H, Zhang K, Yu Q, et al. Enhanced asymmetric circularly polarized luminescence in self-organized helical superstructures enabled

				by macro-chiral liquid crystal quantum dots[J]. ACS nano, 2024, 18(46): 32056-32064.
CsPbX ₃ (X=Cl, Br, I)	±10	±1.5	±1.5	Wang Z, Li A, Cao Q, et al. Processable circularly polarized luminescence for the synthesis of chiral plasmonic nanoparticles[J]. Advanced Optical Materials, 2025, 13(4): 2402310.
CsPbBr ₃	1500	-1500	1.5	Zhang X, Li L, Chen Y, et al. Mechanically tunable circularly polarized luminescence of liquid crystal-templated chiral perovskite quantum dots[J]. Angewandte Chemie, 2024, 136(22): e202404202.
CsPbBr ₃			1.46 and 1.31	Liu T D, Kuo C C, Chang Y C, et al. Ultrabroadband Chiral Emission from Cu Nanocluster Eggshell Membrane/CsPbBr ₃ QD Composites with a Cholesteric Superstructures[J]. Advanced Functional Materials, 2026: e15810.
InP/ZnSeS/Z nS	6000	-30000	0.89	Guo Q, Zhang M, Tong Z, et al. Multimodal-responsive circularly polarized luminescence security materials[J]. Journal of the American Chemical Society, 2023, 145(7): 4246-4253.
InP/ZnSeS/Z nS	10000	-14000	1.0	Zhang M, Gao W, Zhao S, et al. Polymerization-with-assembly enables homogeneous circularly polarized luminescence structures[J]. Nano Research, 2025, 18(7).